Alexandr Volvach et al.: Single Dish Flux Density Monitoring of Geodetic VLBI Sources, IVS 2004 General Meeting Proceedings, p.170–174
http://ivscc.gsfc.nasa.gov/publications/gm2004/volvach

Single Dish Flux Density Monitoring of Geodetic VLBI Sources

Alexandr Volvach [1], *Larisa Volvach* [1], *Yuri Y. Kovalev** [2]

[1)] *Radio Astronomy Laboratory, Crimean Astrophysical Observatory*

[2)] *National Radio Astronomy Observatory*

Contact author: Alexandr Volvach, e-mail: volvach@crao.crimea.ua

Abstract

First campaign of single dish flux density measurements of sources used in geodetic VLBI experiments was carried out at the Simeiz radio telescope. Results of observations at 2.3, 5, and 8.4 GHz are presented and compared with RATAN–600 data.

1. Introduction

Since many compact sources have varying flux, it is important to monitor their correlated flux density in order to schedule geodetic VLBI sessions successfully. For majority of the sources there is a strong correlation between variation of total and correlated flux density [1], therefore single dish measurements can be used for prediction of correlated flux changes. Accompanied with estimates of the correlated flux density derived from analysis of geodetic VLBI observations and with maps produced from analysis of RDV experiments, these time series will provide important information for understanding the physics of these active galactic nuclei.

2. Goals of the Project

The Crimean Astrophysical Observatory has launched an initiative to monitor total flux density of the sources used for geodetic VLBI programs.

Our goal is to provide regular single dish flux density measurements at 2.3, 5, and 8.4 GHz of 104 out of 114 sources from the "geodetic list–2003" visible at the Simeiz radio telescope. Parameters of the instrument are given in Table 1. These sources are scheduled in more than 85% of all geodetic VLBI observations. Each source is observed at least once per month, although many strong sources from this list are scheduled more frequently.

3. Method of Observations and Results

The first campaign was successfully carried out at the Simeiz radio telescope at 2.3, 5, and 8.4 GHz during November 28 — December 11, 2003.

We used a new 5 GHz receiver with the low noise HEMT amplifier (LNA), cooled to a temperature of 15 K and a new dual-band 2.3 and 8 GHz receiver with uncooled LNA. The receivers have been installed in the primary focus of the antenna. Table 2 shows parameters of the receivers and the system equivalent flux density (SEFD).

* also at Astro Space Center of P.N. Lebedev Physical Institute, Moscow, Russia

Table 1. The antenna parameters of the Simeiz station.

Diameter D	22 m
Surface tolerance (root mean square)	0.25 mm
Wavelength limit	2 mm
Feed System	Cassegrian or primary focus
Focal length F	9.525 m
Focal ratio F/D	0.43
Effective focal length for Cassegrian system	134.5 m
Mounting	Alt-Az
Pointing accuracy	10 arcsec
Maximum rotation rate,	1.5 deg/sec
Maximum tracking rate	150 arcsec/sec
Working range in Azimuth (0 to South)	$[-270°, +270°]$
Working range in Elevation	$0° - 85°$

Table 2. Receivers performance and SEFD of the Simeiz antenna.

Band	Band, GHz	$T_{\rm sys}$, K	$T_{\rm receiver}$, K	SEFD, Jy
S	2.1 – 2.5	100	40	1100
C	4.6 – 5.2	35	5	400
X	8.2 – 8.7	80	50	1200

The source antenna temperature was measured by the standard ON–OFF method. Before performing the measurements of each source, we determined the local pointing correction by scanning strong sources. The radio telescope was then pointed alternately on the sources and on the five beam width distance off the source. The source antenna temperature was defined as the difference between the radiometer responses averaged during 10 sec at two different antenna positions. Depending on the intensity of the emission from sources, we made a series of 20–60 measurements and then calculated the mean signal power and the root mean square error of the mean. Four sources, 3C 274, 3C 353, DR–21, NGC 7027, were observed each hour in order to derive gain curves used for calibration. Their flux densities are given by Baars et al. [2] and Ott et al. [3] and form a "standard scale".

Results of flux density measurements at 2, 5 and 8 GHz are presented in Table 3.

We plan to repeat these observations every three months. Each observing campaign at three frequencies takes in total approximately 10 days.

4. Comparison with Other Measurements

We have compared our measurements with 2.3, 3.9, and 7.7 GHz data collected by the Russian 600 meter ring radio telescope RATAN–600 in the second half of 2003 (mainly in October, 2003) in a framework of an ongoing monitoring project with well defined and checked calibration scale

(see description of the program, observations and data reduction procedure in Kovalev et al. [4]). Results of the flux density comparison are presented in Figure 1.

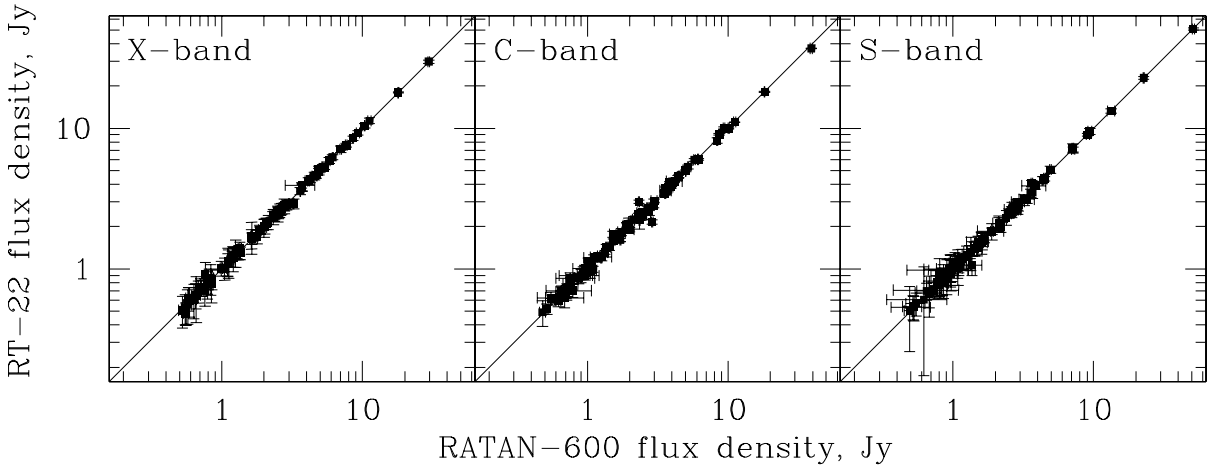

Figure 1. Results of comparison of flux densities measured by RT–22 and RATAN–600 with 1σ error bars.

There is good agreement between the data. A scatter around the line of equality is explained mainly by differences in RT–22 and RATAN–600 bands and by the fact that the sources are variable, but the observations were not strictly simultaneous. We conclude that monitoring observations of the geodetic VLBI sources can be successfully performed by the Simeiz radio telescope RT–22. We expect that further refinement of the methods of observations and data reduction will allow us to reduce random errors of the total flux density measurements.

Acknowledgments. Authors thank I. Srepka for maintenance of the receivers at the station, A. Shevchenko and P. Koseko for their efforts in observations. We are grateful to L. Petrov for useful discussions. RATAN–600 observations were supported in part by the RBFR grant 01–02–16812 and the Russian ministry for science and technology under a subcontract. Y. Kovalev is a Karl Jansky postdoctoral fellow of the National Radio Astronomy Observatory.

References

[1] Kovalev, Y.Y., Kovalev, Yu.A., & Nizhelsky, N.A., In: Future Directions in High Resolution Astronomy, ASP Conf. Ser., in press, 2004.

[2] Baars, J.W.M., Genzel, R., Pauliny-Toth, I.I.K., & Witzel, A., A&A, 61, 99–106, 1977.

[3] Ott, M., Witzel, A., Quirrenbach, A., Krichbaum, T.P., Standke, K.J., Schalinski, C.J., & Hummel, C.A., A&A, 284, 331–339, 1994.

[4] Kovalev, Y.Y., Nizhelsky, N.A., Kovalev, Yu.A., Berlin, A.B., Zhekanis, G.V., Mingaliev, M.G., & Bogdantsov, A.V., A&AS, 139, 545–554, 1999.

Table 3. Results of RT–22 observations of the geodetic VLBI sources in December 2003.

IVS name	IAU name	$S_{8\,\mathrm{GHz}}$, Jy	$S_{5\,\mathrm{GHz}}$, Jy	$S_{2.3\,\mathrm{GHz}}$, Jy
0003−066	0003−066	3.94 ± 0.17	3.05 ± 0.08	2.63 ± 0.17
0048−097	0048−097	0.91 ± 0.19	0.86 ± 0.07	0.76 ± 0.12
0059+581	0059+581	3.80 ± 0.25	3.82 ± 0.05	3.13 ± 0.20
0106+013	0106+013	2.90 ± 0.23	3.44 ± 0.08	3.46 ± 0.23
0111+021	0111+021	0.61 ± 0.11	0.59 ± 0.05	0.53 ± 0.10
0119+041	0119+041	1.01 ± 0.12	0.96 ± 0.08	1.06 ± 0.30
0119+115	0119+115	1.70 ± 0.43	1.59 ± 0.04	1.06 ± 0.16
0201+113	0201+113	0.78 ± 0.21	0.97 ± 0.04	1.03 ± 0.16
0202+149	0202+149	2.00 ± 0.24	2.15 ± 0.08	4.07 ± 0.20
0229+131	0229+131	1.69 ± 0.19	2.04 ± 0.04	1.63 ± 0.19
0235+164	0235+164	1.29 ± 0.13	1.60 ± 0.04	1.85 ± 0.09
3C 84	0316+413	17.96 ± 0.15	18.17 ± 0.19	22.82 ± 0.44
CTA 26	0336−019	2.60 ± 0.19	2.82 ± 0.09	2.89 ± 0.21
NRAO 150	0355+508	5.90 ± 0.29	3.74 ± 0.09	2.77 ± 0.12
0434−188	0434−188	0.84 ± 0.13	0.99 ± 0.05	1.10 ± 0.20
0454−234	0454−234	3.58 ± 0.21	3.60 ± 0.08	2.67 ± 0.19
0458−020	0458−020	1.17 ± 0.15	1.21 ± 0.05	1.17 ± 0.20
0528+134	0528+134	2.86 ± 0.22	2.70 ± 0.08	2.32 ± 0.27
0552+398	0552+398	4.93 ± 0.27	4.99 ± 0.06	3.00 ± 0.16
0556+238	0556+238	0.60 ± 0.16	0.69 ± 0.07	0.98 ± 0.16
0607−157	0607−157	4.65 ± 0.24	4.09 ± 0.08	2.64 ± 0.33
0642+449	0642+449	4.23 ± 0.23	3.00 ± 0.07	0.99 ± 0.18
0656+082	0656+082	0.53 ± 0.12	0.62 ± 0.09	0.80 ± 0.16
0727−115	0727−115	5.10 ± 0.26	4.50 ± 0.10	3.50 ± 0.32
0743+259	0743+259	0.48 ± 0.08	0.69 ± 0.09	1.01 ± 0.28
0804+499	0804+499	0.65 ± 0.13	0.70 ± 0.06	0.79 ± 0.14
0805+410	0805+410	0.80 ± 0.09	0.61 ± 0.06	0.70 ± 0.09
0808+019	0808+019	0.74 ± 0.10	0.68 ± 0.06	0.69 ± 0.09
0823+033	0823+033	1.31 ± 0.29	1.19 ± 0.07	1.00 ± 0.15
OJ 287	0851+202	2.60 ± 0.19	2.04 ± 0.09	1.54 ± 0.27
4C 39.25	0923+392	10.41 ± 0.39	9.07 ± 0.10	5.08 ± 0.29
OK 290	0953+254	0.86 ± 0.21	0.94 ± 0.09	1.00 ± 0.26
0955+476	0955+476	1.87 ± 0.12	1.70 ± 0.06	1.10 ± 0.12
1034−293	1034−293	1.14 ± 0.26	1.00 ± 0.05	0.67 ± 0.21
1101+384	1101+384	0.55 ± 0.15	0.52 ± 0.04	0.84 ± 0.22
1124−186	1124−186	1.64 ± 0.26	1.42 ± 0.07	1.07 ± 0.20
1128+385	1128+385	1.40 ± 0.14	1.20 ± 0.05	0.60 ± 0.43
1156+295	1156+295	1.90 ± 0.13	1.90 ± 0.06	1.85 ± 0.24

Table 4. Results of RT–22 observations of the geodetic VLBI sources in December 2003.

IVS name	IAU name	$S_{8\,\mathrm{GHz}}$, Jy	$S_{5\,\mathrm{GHz}}$, Jy	$S_{2.3\,\mathrm{GHz}}$, Jy
1219+044	1219+044	0.69 ± 0.12	0.77 ± 0.07	0.67 ± 0.14
3C 273B	1226+023	29.80 ± 0.73	37.01 ± 0.21	50.98 ± 0.90
1300+580	1300+580	0.78 ± 0.12	0.85 ± 0.07	0.54 ± 0.10
1302−102	1302−102	0.50 ± 0.12	0.70 ± 0.07	1.00 ± 0.24
1308+326	1308+326	2.40 ± 0.22	2.00 ± 0.10	1.09 ± 0.15
1334−127	1334−127	3.80 ± 0.22	3.70 ± 0.22	2.85 ± 0.22
1351−018	1351−018	0.78 ± 0.17	0.90 ± 0.07	0.98 ± 0.17
OQ 208	1404+286	2.14 ± 0.24	2.21 ± 0.29	1.66 ± 0.12
1418+546	1418+546	1.01 ± 0.18	1.02 ± 0.17	0.83 ± 0.18
1519−273	1519−273	2.51 ± 0.23	2.09 ± 0.21	1.56 ± 0.14
1606+106	1606+106	1.97 ± 0.29	2.40 ± 0.15	2.59 ± 0.18
1611+343	1611+343	5.31 ± 0.23	4.57 ± 0.11	4.39 ± 0.15
1622−253	1622−253	4.57 ± 0.27	4.20 ± 0.08	2.51 ± 0.14
NRAO 512	1638+398	1.09 ± 0.19	1.21 ± 0.07	1.32 ± 0.35
3C 345	1641+399	7.58 ± 0.25	8.19 ± 0.37	9.04 ± 0.20
DA 426	1652+398	1.65 ± 0.15	1.68 ± 0.12	1.39 ± 0.15
1726+455	1726+455	1.22 ± 0.19	1.10 ± 0.09	1.08 ± 0.19
1739+522	1739+522	1.29 ± 0.11	1.23 ± 0.07	1.09 ± 0.13
1741−038	1741−038	6.21 ± 0.25	5.32 ± 0.17	4.30 ± 0.25
1745+624	1745+624	0.73 ± 0.09	0.67 ± 0.07	0.56 ± 0.10
1749+096	1749+096	2.60 ± 0.28	1.76 ± 0.08	1.22 ± 0.23
1908−201	1908−201	2.35 ± 0.29	2.35 ± 0.07	2.13 ± 0.18
1920−211	1920−211	2.43 ± 0.28	2.60 ± 0.20	3.09 ± 0.27
1921−293	1921−293	11.32 ± 0.55	10.04 ± 0.23	9.50 ± 0.46
1923+210	1923+210	2.40 ± 0.15	1.82 ± 0.10	1.41 ± 0.17
1958−179	1958−179	2.69 ± 0.24	2.24 ± 0.11	1.32 ± 0.14
2113+293	2113+293	0.59 ± 0.14	0.49 ± 0.10	0.50 ± 0.24
2121+053	2121+053	2.53 ± 0.18	2.47 ± 0.07	2.01 ± 0.20
2126−158	2126−158	1.31 ± 0.15	1.31 ± 0.04	0.92 ± 0.22
2128−123	2128−123	4.35 ± 0.23	4.02 ± 0.14	2.88 ± 0.29
2134+00	2134+000	8.49 ± 0.31	10.01 ± 0.08	7.08 ± 0.29
2136+141	2136+141	2.76 ± 0.19	2.43 ± 0.06	1.57 ± 0.20
2145+067	2145+067	7.10 ± 0.37	5.98 ± 0.13	3.91 ± 0.21
2149+056	2149+056	0.69 ± 0.15	0.89 ± 0.09	0.90 ± 0.28
2201+315	2201+315	2.80 ± 0.34	2.50 ± 0.05	2.10 ± 0.27
2209+236	2209+236	0.65 ± 0.23	0.89 ± 0.05	1.27 ± 0.27
3C 446	2223−052	5.30 ± 0.22	6.00 ± 0.07	7.20 ± 0.55
2234+282	2234+282	1.19 ± 0.24	1.42 ± 0.07	1.50 ± 0.29
2243−123	2243−123	2.10 ± 0.20	2.35 ± 0.14	2.48 ± 0.18
3C 454.3	2251+158	9.29 ± 0.31	11.08 ± 0.05	13.29 ± 0.47
2255−282	2255−282	5.01 ± 0.26	3.43 ± 0.05	2.70 ± 0.37
2318+049	2318+049	1.11 ± 0.25	1.06 ± 0.09	0.90 ± 0.25
2356+385	2356+385	0.45 ± 0.13	0.56 ± 0.10	0.43 ± 0.09